NOLTR 61-83

NOX

FREE FLIGHT EXPERIMENTAL INVESTIGATIONS OF THE EFFECT OF BOUNDARY LAYER COOLING ON TRANSITION

29 SEPTEMBER 1961

NOL

UNITED STATES NAVAL ORDNANCE LABORATORY, WHITE OAK, MARYLAND

NOLTR 61-83

Ballistics Research Report 46

FREE FLIGHT EXPERIMENTAL INVESTIGATIONS OF THE EFFECT OF BOUNDARY LAYER COOLING ON TRANSITION

Prepared by:

W. C. Lyons, Jr. and Norman W. Sheetz, Jr.

ABSTRACT: Free flight tests have been conducted in the NOL Pressurized Ballistics Range No. 3 for the purpose of investigating boundary layer transition under the conditions of extreme boundary layer cooling. The tests were conducted on smooth, sharp-nosed, slender cones. The tests were conducted at a nominal Mach number of 3 and a free stream unit Reynolds number per foot of 11.8×10^6. The ratio of wall to adiabatic recovery temperature varied between 0.22 and 0.27. The results of the tests agreed very closely with results from wind tunnel tests conducted at similar conditions. These free flight tests seem to substantiate earlier results which indicate a destabilizing trend for laminar boundary layers subjected to extreme cooling.

U. S. NAVAL ORDNANCE LABORATORY
WHITE OAK, MARYLAND

NOLTR 61-83 29 September 1961

FREE FLIGHT EXPERIMENTAL INVESTIGATIONS OF THE EFFECT OF BOUNDARY LAYER COOLING ON TRANSITION

This report presents the results of free flight tests conducted in a ballistics range at the Naval Ordnance Laboratory to determine the effect of extreme boundary layer cooling on transition. The results from these tests are compared with results from wind-tunnel tests conducted at comparable conditions. The results are also compared with presently available boundary layer stability theories.

The work was performed under Task Number 803-767/73001/03-073 for the Bureau of Naval Weapons.

Although many persons contributed to this research program, the authors wish to express their appreciation to Mr. Harry A. Feather who designed the final version of the sabot used in these tests. Acknowledgement is also extended to Miss Amy A. Chamberlin for her assistance in performing much of the data reduction and to Mr. Hensel S. Brown who coded the various computational programs for use on the IBM-704.

W. D. COLEMAN
Captain, USN
Commander

A. E. SEIGEL
By direction

CONTENTS

ILLUSTRATIONS

TABLES

SYMBOLS

A, C	constants
C_f	local skin friction coefficient
C_H	Stanton number
C_p	specific heat at constant pressure
h	local heat transfer coefficient
k	surface roughness height
M	Mach number
P	static pressure
r	temperature recovery factor
Re	Reynolds number
R_{e_k}	Reynolds number based on surface roughness height and flow conditions evaluated at the top of the roughness
$R_{e_{tr}}$	Reynolds number based on distance from vertex of model to the location of transition and flow conditions evaluated at the point of transition
T	temperature
T_r	adiabatic recovery temperature
T_w	wall temperature of the model
U	flow velocity
X	direction along surface of model
X_{tr}	distance along surface of model to location of transition
y	direction normal to model surface
α	yaw angle
γ	ratio of specific heats
δ^*	boundary layer displacement thickness

SYMBOLS

δ_H	horizontal projection of yaw angle
δ_V	vertical projection of yaw angle
μ	coefficient of fluid viscosity
ξ	direction along centerline of model
ρ	density

Subscripts

B	free stream conditions within the heated section of the range
e	conditions at the edge of the boundary layer
k	conditions within the boundary layer evaluated at a height "k"
l	laminar
m	physical properties of the model
t	turbulent

FREE FLIGHT EXPERIMENTAL INVESTIGATIONS OF THE EFFECT OF BOUNDARY LAYER COOLING ON TRANSITION

INTRODUCTION

1. The importance of accurately predicting boundary layer transition is illustrated by the large amount of effort expended in the study of this phenomenon. The apparent large number of parameters which significantly affect transition increases the difficulty encountered in either a systematic theoretical or experimental study of transition. Among the many parameters to be considered is the rate heat is transferred from the boundary layer to the body or vice versa. A theoretical study reported by Van Driest (reference (a)) indicates that a stabilizing effect on the boundary layer results with increased heat transfer from the boundary layer to the body. It was further determined in reference (a) and also indicated in reference (b) that at certain Mach numbers, the laminar boundary layer can be completely stabilized by the presence of an appropriate amount of cooling of the boundary layer regardless of the Reynolds number.

2. A large amount of experimental evidence exists which substantiates this stabilizing effect for moderate rates of cooling (see references (c), (d), (e), and (f)). More current experimental investigations of the effect of extreme cooling on boundary layer transition have revealed a reversal in the movement of the location of transition for decreasing values of the ratios of wall to adiabatic recovery temperature (references (g) and (h)). Experimental data from reference (h) indicate that for moderate cooling, the transition Reynolds number increased with decreasing values of the ratio of wall to adiabatic recovery temperature down to a value of Tw/Tr of approximately 0.52. Further decreases in this temperature ratio resulted in a large decrease in transition Reynolds number. The small values of Tw/Tr that were obtained in the tests described in reference (h) were accomplished by cooling the surface of the model to very low temperatures (approximately -340°F). As a result of these very low wall temperatures, air components such as oxygen, carbon dioxide, and water vapor could condense on the cold surface and thereby generate a surface roughness. Whether the presence of this condensation film produces sufficient surface roughness to cause the transition reversal effect or not is questionable. It is, however, an undesirable condition to exist during a transition study.

3. The present program consisted of launching 10-degree total angle, sharp-nosed cones in the NOL Pressurized Ballistics Range No. 3. The ambient temperature in a portion of the range was varied so that different adiabatic recovery temperatures could be obtained at a constant, nominal Mach number of 3.1. The location of transition on the models was obtained during flight from spark shadowgraph photographs for temperature ratios, Tw/Tr, between 0.22 and 0.27. The surface temperature of the models varied only slightly from room temperature ($534^{\circ}R$) during the tests. Using this technique of increasing the recovery temperature rather than decreasing the wall temperature to obtain the condition of "extreme cooling" (temperature ratios, Tw/Tr, comparable to those obtained in reference (h)) alleviated the possibility of a condensate film forming on the models and therefore preserved a very smooth testing surface. The present experimental program paralled very nearly the tests reported in reference (h) (approximately the same free stream Mach number, free stream Reynolds number per foot, external model geometry, and temperature ratios Tw/Tr). By eliminating or at least reducing factors such as surface roughness and free stream turbulence, it was considered that boundary layer transition measurements would be more significant, especially in attempting to determine the parameters which contribute to the transition reversal phenomena.

DESCRIPTION OF EXPERIMENTS

NOL Pressurized Ballistics Range No. 3

4. The transition tests being reported were conducted in the NOL Pressurized Ballistics Range No. 3 (reference (i)). This range consists of an enclosed steel tube, three feet in diameter and three hundred feet long. A gun is mounted at one end of the tube and the model is normally caught in a sand butt at the other end. Figure 1 is a photograph of the Pressurized Ballistics Range No. 3.

5. The test unit Reynolds number within the range can be controlled through a variation in the range pressure. This is accomplished by pumps connected to the range. These pumps permit pressurization up to about 6 atmospheres or evacuation down to 1/100 atmosphere. The air temperature in both the range and the room housing the range is normally maintained at 74 $\pm$ 1 degrees Fahrenheit.

6. Although a variety of sizes and types of guns are available for use with the Pressurized Ballistics Range No. 3, a 40-mm powder-charged, smooth bore gun was used for these tests. This gun had previously exhibited a high degree of reliability and permitted a Mach number of 3 to be attained with the size models used in these tests.

7. The Pressurized Ballistics Range No. 3 is equipped with twenty-five spark-shadowgraph stations. Spark shadowgraphs of the models were made at each of the stations during a flight although, as will be discussed in detail later in this report, only four stations were used to obtain the data that is being presented. The location of transition was determined by a visual inspection of each of the shadowgraph plates.

Heating Box

8. To obtain the desired small values of Tw/Tr for the model flights at a Mach number of 3, a steel box was constructed which could be placed in the range. The air within this box could be heated up to approximately 900°R. Heating the air through which the models flew during the portion of their flight within the box allowed the necessary recovery temperatures to be attained at the test Mach number of approximately 3.

9. Baffle plates which are located in the Pressurized Ballistics Range No. 3 between spark-shadowgraph stations have openings in them approximately thirteen inches square through which the models must pass during their flight down the range. The size of these openings in the baffle plates required that the cross-sectional area of the heating box be limited to one square foot. It was decided to obtain transition data from the models while flying in the heated air at four consecutive spark shadowgraph stations. To accomplish this, it was necessary to construct a box twenty-two feet long. Since instrumentation associated with the spark shadowgraph stations was external to the box, windows were required so that the model could be viewed while flying through the box by the photographic equipment. Sixteen 1/4-inch plate glass windows were located in the box to correspond with the location of the four data stations. The box was fabricated from 1/16-inch steel and was thermally insulated by a 1/4-inch layer of asbestos composition on the inside and by a one-inch layer of asbestos composition with an aluminum foil covering on the outside. To facilitate heating and retaining air captured within the box, quick opening doors were installed at each end of the box. The ends of the box could be opened by dropping these doors vertically downward. The doors could be released remotely outside the range by solenoid operated latch mechanisms. A sketch of the heating box installed in the range is presented in Figure 2.

10. The air within the box was heated by means of General Electric "Calrod" tubular heaters. Two heating rods extended the length of the box in each of the four corners of the box. This arrangement of heaters was chosen so that sufficient heat could be supplied to the air and so that an even distribution of air temperature within the box could be attained. Also, to obtain an even temperature distribution of the air throughout the interior of the box, and also to create a method for obtaining and controlling the required air temperature within the box, the "Calrod" heaters were divided into four equal sections down the length of the box. The power supplied to each of these sections was individually controlled by means of a transformer. This allowed a variation in the power supplied to each section. These transformers, in conjunction with a 220-volt AC power supply fused for 60 amperes, provided a continuously variable voltage from 0 to 270 volts which could be applied across each heater section.

11. The temperature of the air within the box was measured during a test by twelve thermocouples, six along the top of the box and six along the bottom of the box. The location of these thermocouples is illustrated in Figure 2. It was found that by proper adjustment of the transformers, the temperature variation along the length of the box could be maintained constant within approximately ± 2 degrees. To determine the temperature distribution throughout the cross-section of the box, a thermocouple probe was designed for surveying the air temperature along a vertical plane in the center of the box. Several surveys were made during bench tests of the box prior to installation in the ballistics range. This survey, which was conducted at various positions along the length of the box, revealed that a temperature variation of approximately 10 degrees existed in a layer extending about one inch from the walls. Other than this thin thermal layer on the walls, the temperature distribution along this vertical line at any survey station was constant to within one degree.

Models and Sabots

12. Although two different types of models were used in these tests, for the purpose of analyzing the data, they could be considered identical. Both types of models consisted of 10-degree total angle, sharp-nosed cones. The base diameter of both models was 1.20 inches. The difference in the two models existed in a ½-inch cylindrical extension to the base of the cone which appears on models which will be referred to as Type A and which is absent on models referred to as Type B. Sketches of these models are presented in Figure 3. The models were hollow in the aft end to provide a center of gravity as far forward as possible. This provided a model with a sufficiently large static margin to produce a reliable flight trajectory.

13. The models were fabricated from Graph-Mo tool steel and hardened to a Rockwell C of approximately 35. To obtain a sharp tip and a very smooth surface finish, the final manufacturing process was grinding. Previous experience in conducting transition programs in the ballistics range at NOL (reference (j)) indicated that a more uniform surface finish could be obtained by simply grinding Graph-Mo steel rather than by polishing. Further, it is very difficult to maintain a straight surface free from waves when polishing is attempted. By grinding, a surface finish was obtained on the models which varied between 1.5 and 5.5 microinches root mean square with most of the models having a surface roughness of approximately 3 microinches root mean square. The surface roughness measurements were made using a Taylor-Hobson "Talysurf" recorder. To determine if the surface roughness was uniform along the length of the cones, a model was chosen at random and measurements were made at four positions along the length. From these measurements, it was determined that the roughness did not vary significantly along the length of the model. To facilitate subsequent surface roughness measurements and also to eliminate any surface aberration resulting from the diamond measuring stylus of the Talysurf recorder, typical roughness measurements were made only at one position on the aft portion of the lateral surface of each model. Typical surface roughness measurement records produced by the Talysurf recorder are presented in Figure 4. To insure that the nose of each model that was tested was straight and sharp, a 100 magnification photograph was taken of the model nose prior to launching. To illustrate a typical model nose, one of these photographs is presented in Figure 5.

14. The sabots which were used to position the models in the barrel of the gun during the launching process were fabricated from fine linen base phenolic. Initial attempts were made to launch the models using a sabot which gripped the model over a very small area at the aft end of the model and did not touch any of the other surface of the model. These attempts, however, were not successful since large angles of initial yaw occurred during these tests. A different sabot was designed which gripped the model continuously from the base of the cone to a point 4.83 inches from the vertex of the cone. Figure 6 is a photograph of a typical model and sabot of this latter described design. It was found that by using a sabot designed as illustrated in Figure 6, reliable, low angle of yaw launchings could be obtained. Although it was initially assumed that the sabot touching the surface of the model would have negligible effect upon the roughness of

the surface, tests were performed to obtain qualitative justification of this assumption. To perform these tests, a flat plate of Graph-Mo was fabricated with a ground surface equivalent in surface roughness to the transition models. The surface roughness of this plate was measured and recorded using the Talysurf recorder. Following this measurement, the plate was impacted and violently scraped with samples of the sabot material. After this severe treatment of the plate a second measurement of the surface roughness was made and recorded using the Talysurf recorder. As can be seen from the Talysurf records presented in Figure 7, no discernible surface effects could be detected due to these impact and abrasion tests.

TEST PROCEDURE

15. During the process of conducting the transition tests the following procedure was used. The end doors of the heating box were closed and secured by means of the solenoid operated latches. The heaters in the box were then energized and the confined air was heated to approximately the desired uniform temperature which had been previously selected for a particular launching. Depending upon this desired temperature, this heating process required up to two hours. When the approximate desired air temperature was achieved, the model and sabot were loaded into the gun and the range was closed and sealed. Vacuum pumps were then used to evacuate the range and obtain the desired range test pressure. The pressure selected for a test was that pressure which would result in a unit Reynolds number per foot within the heated box of approximately 11.8 million. This is near the Reynolds number per foot which existed during the tests reported in reference (h). Also, it has been determined that this Reynolds number per foot would permit the largest variation in the temperature ratio Tw/Tr while having transition occur on the model. After obtaining the desired range pressure, a final adjustment was made to the heater power so that the air temperature within the box was as uniform as possible and had the correct magnitude as indicated by the twelve permanently installed thermocouples. After these final adjustments to the air temperature were made, the end doors of the heating box were opened approximately 5 seconds before launching the model in the range.

DATA REDUCTION PROCEDURES

16. The location of transition on the model was determined from spark shadowgraph photographs of the model during its flight down the range. The photographic plates consisted of

a film emulsion on a 14 by 17-inch glass plate. At each data station, photographs of the model were obtained in both the vertical and horizontal planes although only the vertical photographs provided sufficient detail of the flow field and the boundary layer to determine where the boundary layer was laminar and where it was turbulent. Depending upon the location of the model between the light source and the photographic plate, the magnification of the model by the optical system can vary from 1 to 1.3 times its actual size. The magnification of the model on each photographic plate was measured by comparing the size of the image to the true size of the model. The location of transition was measured from the nose of the image directly from the glass photographic plate. This length was multiplied by the magnification factor for the plate to obtain the actual location of transition on the model. Three independent measurements were made for each plate and the location of transition was taken as the arithmetical mean of these measurements. A typical spark shadowgraph photograph of a model flying in the range is presented in Figure 8.

17. The velocity, Mach number, and angle of attack were obtained through a visual observation of the shadowgraph plates and a standard data reduction program described in reference (k).

18. The recovery temperature of the air in the heated section of the range was obtained from the equation:

$$T_r = T_B\left(1 + r\frac{\gamma-1}{2}M_B^2\right) \qquad (1)$$

The recovery factor, r, was assumed to be 0.85 in the laminar region and 0.88 in the turbulent region. These values agree with experimental values obtained in wind-tunnel experiments on 10^0 cones at Mach numbers of approximately 3 described in references (l), (m), and (n).

19. The surface temperature of the cone was calculated with the aid of an IBM-704 computer. The results of a typical calculation are shown in Figure 9. The method of calculation is presented in Appendix A.

20. The Reynolds number based upon distance from the nose of the model to the location of transition was chosen as a parameter to indicate the degree of stability of the boundary layer. Both free stream and local transition Reynolds numbers

were calculated. The free stream Reynolds number based on length of laminar flow is:

$$R_{e_{tr}}|_B = \frac{\rho_B U_B X_{tr}}{\mu_B} \tag{2}$$

Upon introducing Sutherland's viscosity law and the equation of state for a perfect gas, the above may be rewritten as:

$$R_{e_{tr}}|_B = A \frac{P_B U_B X_{tr}}{T_B^{5/2}} (T_B + C) \tag{3}$$

P_B was measured by pressure gages attached to the Pressurized Ballistics Range No. 3. The velocity was determined at each data station by measuring the time required for the model to travel from one data station to another. Thermocouples were placed at the top and bottom of the heating box, directly before and after each data station within the heated section of the range, to measure the free stream ambient temperature at the station. X_{tr} was obtained from observation of the shadowgraph pictures of the model in flight.

21. The local Reynolds number based on the length of laminar flow is:

$$R_{e_{tr}}|_e = \frac{\rho_e U_e X_{tr}}{\mu_e} \tag{4}$$

After Sutherland's viscosity law and the equation of state for a perfect gas are introduced, equation (4) may be written as:

$$R_{e_{tr}}|_e = A \frac{P_e U_e X_{tr}}{T_e^{5/2}} (T_e + C) \tag{5}$$

The local properties that appear in equation (5) were calculated with the aid of tables of flow properties for yawed cones (reference (o)) and tables of isentropic flow (reference (p)). X_{tr} was obtained from shadowgraph pictures.

22. Reference (o) describes the flow field around a yawed cone as being constant along elements of the cone. However, since the model flew with yaw in both the vertical and horizontal planes in the general case, it was necessary to determine just which elements of the cone were seen in the shadowgraph plates.

23. In order to determine the flow conditions at the transition point seen on the windward and leeward sides of the vertical shadowgraph, it was necessary to calculate the angular displacement of these elements from the meridian plane. The flow conditions can then be obtained along the conical element from the tables in reference (o).

DISCUSSION OF RESULTS

24. An objective of this program was to eliminate some of the undesirable conditions which were inherent in the experimental techniques employed in previous tests in which the transition reversal phenomenon was observed. Two of these conditions, which have an undetermined effect on the location of transition, are free stream turbulence associated with wind tunnel tests, and an undesired surface roughness created by the condensation of air on very cool model walls. The first of these conditions was eliminated by conducting the present tests in a ballistics range where the free stream turbulence is essentially zero. The second condition was eliminated by creating a highly cooled boundary layer by increasing the recovery temperature of the air rather than by cooling the walls of the model and thereby eliminating any possibility of the formation of frost or condensate on the model surface.

25. The data obtained during these tests are presented in Table I as transition Reynolds numbers based on both free stream conditions in the undisturbed air and local conditions just outside of the boundary layer. The length used in these Reynolds numbers was that distance measured along the surface of the cone between the vertex of the cone and the point where the boundary layer became turbulent and remained turbulent. In many instances it was noted that turbulent bursts appeared on the model. These turbulent bursts were small regions of turbulent flow which would be followed by laminar flow. The occurrence of turbulent bursts on a highly polished cone used in a series of ballistics range tests was reported by Witt (reference (j)). The observance of turbulent bursts on a slender body of revolution (ogive-cylinder) also used in a series of ballistics range tests was reported by Jedlicko, et. al., (reference (q)). An analysis presented in reference (q) indicated that bursts could probably be a result of surface roughness, especially near the tip of the model. Referring to Figure 5 it is seen that there is a very slight aberration of the tip and upon reviewing the photographs of the tips of the other models used in this program there were no model tips found with a more severe aberration. These tip imperfections are negligible when compared to the size of imperfection considered by Jedlicko, et. al., (reference (q)), who presented a photograph of a model tip which had been bent off the model axis 0.003 inch. No indication was given, however, concerning the minimum size imperfection necessary to initiate a turbulent burst. A spark shadowgraph photograph of a transition model on which turbulent bursts occur is presented in Figure 10.

26. It will be noted from the data presented in Table I that normally information was obtained from only one or two stations for each shot. In one instance (Shot No. 4050) data were obtained from three stations. When spark shadowgraph photographs were taken while the model was in the heating box, light from the spark source passed through two plate glass windows in the box and therefore some attenuation of the light occurred. Photographs in the vertical plane are made in the Pressurized Ballistics Range No. 3 by exposing the plates directly with light from the spark source while photographs in the horizontal plane are exposed by indirect light from the same spark source. This light is redirected to expose the horizontal plates by means of a mirror. Due to an attenuation of the light by this mirror, horizontal plates produce a consistently lower quality photograph than do the vertical plates. It was the additional attenuation of light by the two horizontal plate glass windows that made it impossible to obtain distinct pictures of the flow pattern over the cones in a horizontal plane and therefore transition data were obtained from vertical plates only. Since the light to the vertical plates was also attenuated by the vertical windows, it was essential that each photographic plate be correctly exposed to produce a picture in which the flow field and boundary layer were sufficiently distinct to allow the location of transition to be determined. This was the primary reason for not obtaining and presenting data for all of the stations within the box for every shot. A few plates were also lost from time to time due to malfunctioning of electronic equipment and associated instrumentation.

27. It is impossible to maintain a specified angle of yaw of a model during its flight in a ballistics range test. For the tests being reported, an extensive effort was made to design a model-sabot combination which would result in small initial yaw angles and consequently the models would have a small angle of attack during its flight. The data in this report were obtained from launchings that resulted in angles of yaw of the model while in the heating box of less than 4.5 degrees. In Table I the vertical (δ_V) and horizontal (δ_H) projections of the angle of yaw (α) are presented for each data point. For small values of δ_V and δ_H (δ_V and $\delta_H < 5$ degrees) the angle of yaw is given approximately by $\alpha^2 = \delta_V^2 + \delta_H^2$.

28. As a result of the motion of the cone models as they flew down the range the orientation of the meridian plane (that plane defined by the velocity vector of the center of gravity of the model and the longitudinal centerline of the model) continually changed. This can easily be visualized by

considering the yawing[1] motion of a body in flight in which this motion is not planar. Since the location of transition was obtained from photographic plates placed vertically in the range, the two rays on the surface of the cone on which transition is seen continually vary with time in angular position with respect to the most windward ray in the meridian plane. This factor accounts, in part, for the variation of the location of transition on the apparent windward and leeward ray of a model flying down the range as viewed in the spark shadowgraph photographs. Since the temperature ratio, Tw/Tr, remains essentially constant during a flight, there results some large variations in the location of transition for approximately the same temperature ratio. Some of the effect of angle of yaw was minimized by expressing the location of transition in terms of a transition Reynolds number base on local flow properties on the yawed cone at the point of transition and the length of the laminar region measured from the vertex of the cone. The transition data obtained from these tests are presented in Figure 11 as the local transition Reynolds number plotted as a function of the temperature ratio, Tw/Tr, at transition. The solid curves were taken from Figure 3 of reference (h). These solid curves represent experimental data obtained during wind-tunnel tests over a range of boundary layer cooling from moderate to extreme cooling. Even though there are effects of angle of yaw reflected in the scatter of the data obtained during the free flight tests, an agreement of these data with the data obtained in a wind tunnel and reported in reference (h) is obvious. Although there is a slight slope to the curve presented in reference (h), the scatter of the free flight data makes it impossible to determine a meaningful curve from these data. In fact, it would appear that the transition Reynolds number has very little dependency on the temperature ratio at the values of Tw/Tr obtained during the present tests. It is apparent, however, that the free flight data represented by the points in Figure 11 cannot be associated with the upper curve and therefore some destabilizing effects appear to be present at the conditions of extreme cooling that are not significant for the condition of moderate cooling.

29. Since the boundary layer tends to become thinner with increased cooling, the ratio of roughness height, h, to boundary layer thickness, δ , becomes larger with cooling.

---

[1] In this report the yawing motion refers to the resultant angular motion of the model about vertical and horizontal transverse axes passing through the center of gravity of the model and not the angular motion about just one of the transverse axes as the term yaw often implies.

This would indicate that the effect of a particular size roughness element would become more pronounced with increased cooling. As was stated in paragraph 13, the roughest model used in these tests had a centerline average roughness of 5.5 microinches rms. An investigation of all of the Talysurf roughness traces revealed a few discrete roughness protuberances as large as 30 microinches. Boundary layer characteristics were computed along the bodies of the models so that a comparison of roughness height and boundary layer thickness could be made. In Figure 12 the momentum thickness and the displacement thickness for a typical flight condition experienced during these tests are plotted as a function of the distance along the centerline of the model. A comparison of the largest protuberance height, k, found on any of the models (30 microinches) to the boundary layer displacement thickness, δ^*, indicated a ratio of $k/\delta^* = .015$. It has been established by a number of investigators (see references (r) and (s)) that the critical roughness height required to initiate turbulence can be expressed in terms of a critical roughness Reynolds number which is approximately constant for all speed ranges. This critical Reynolds number is based on local conditions at the top of the roughness. As indicated in reference (r), for three-dimensional roughness at a Reynolds number less than its critical value, the roughness introduces no disturbances of sufficient magnitude to influence transition. The Reynolds number based on conditions at the top of the roughness can be expressed as:

$$R_{e_k} = A\, P_k U_k \frac{(T_k + C)}{T_k^{5/2}} K \times 10^4$$

where P is the pressure, U is the velocity, T is the temperature, k is the height of the protuberance, and A and C are constants. The subscript, k, indicates that the quantities are to be evaluated at the top of the protuberance. Since it is assumed that $\partial P/\partial y = 0$ (where y is the direction normal to the surface) then $P_k = P_e$ where the subscript e indicates local condition just outside of the boundary layer. Further it can be shown that

$$U_k < U_e \quad \text{and} \quad T_k > T_w.$$

If the local pressure and velocity and the wall temperature are substituted for the pressure, velocity, and temperature at the top of the roughness, respectively, then the resulting

Reynolds number will be a maximum and is expressed as

$$Re_{MAX} = A P_e U_e \frac{T_W}{T_W^{5/2}} \frac{C}{k}$$

Values for $R_{e\ max.}$ were computed for each data point assuming $k = 30$ microinches. The maximum value computed was $R_{e\ max.} = 84.$ Values for the critical roughness Reynolds numbers were obtained experimentally on a cooled 10° total angle cone and reported in reference (r). These results indicated that the value for $R_{e\ critical} \cong 400$. It can be seen that values of $R_{e\ max.}$ are well below the values of $R_{e\ critical}$ reported in reference (r).

30. It was decided to compare the data obtained from these free flight experiments with one of the theories which predict the limits of infinite stability of the boundary layer. The theory reported by Van Driest (reference (b)) was used for this comparison. Although the region of infinite stability is often presented as a plot of the ratio of wall to local temperature just outside the boundary layer versus local Mach number, in Figure 13, the region is presented as a plot of the ratio of wall to recovery temperature versus the local Mach number. Since all of the data being presented were obtained at a constant Mach number and over a relatively small range of temperature ratios, they appear merely as a short vertical line in Figure 13. It is interesting to note that although transition was occurring on the cone, the conditions at which the tests were being conducted indicated that the boundary layer was well within the theoretical region of infinite stability.

CONCLUSION

31. Tests have been conducted in a ballistics range which definitely support the occurrence of the phenomenon referred to as "transition reversal." These tests were conducted at conditions which parallel previously conducted wind-tunnel tests and the agreement between the data obtained during the wind-tunnel tests and the ballistics range tests was extremely good.

32. An effort was made to minimize the effect of surface roughness as a possible cause of the reversal trend of the

movement of transition with a variation of the ratio of wall to recovery temperature. A stringent analysis of the data and the model and flight conditions at which the data were obtained indicated that it was extremely unlikely that physical surface roughness was the primary cause of the transition reversal phenomenon. Although the angle of yaw of the models influenced the location of transition, it does not appear that this had a significant effect on the location of transition.

33. The data obtained in this program and presented graphically as the temperature ratio, Tw/Tr, versus transition Reynolds number indicate that the relatively large variation in transition Reynolds numbers may not be a result of the variation of the temperature ratio in the region of temperature ratios investigated during this program.

34. It appears that additional information will have to be obtained to conclusively determine the cause of this phenomenon.

REFERENCES

(a) Van Driest, E. R., "Calculation of the Stability of the Laminar Boundary Layer in Compressible Fluid on a Flat Plate with Heat Transfer," Journal of the Aeronautical Sciences, Vol. 19, No. 12, December 1952

(b) Van Driest, E. R., "The Laminar Boundary Layer with Variable Fluid Properties," Report No. AL-1866, North American Aviation, Inc., Downey, California, January 1954

(c) Van Driest, E. R., and Boison, J. C., "Research on Stability and Transition of the Laminar Boundary Layer," Report No. AL-2196, North American Aviation, Inc., Downey, California, September 1955

(d) Browning, A. C.; Crane, J. F. W.; and Monaghan, R. J., "Measurements of the Effect of Surface Cooling on Boundary Layer Transition on a 15° Cone," (Part I) Technical Note No. Aero-2527, Royal Aircraft Establishment, Farnborough, September 1957

(e) Czarnecki, K. R., and Sinclair, C. R., "An Extension of the Investigation of the Effects of Heat Transfer on Boundary Layer Transition on a Parabolic Body of Revolution (NACA RM-10) at a Mach Number of 1.61," NACA TN 3166, April 1954

(f) Higgins, R. W., and Pappas, C. C., "An Experimental Investigation of the Effect of Surface Heating on Boundary Layer Transition on a Flat Plate in Supersonic Flow," NACA TN 2351, April 1951

(g) Diaconis, N. S.; Wisniewski, R. J.; and Jack, J. R., "Heat Transfer and Boundary Layer Transition on Two Blunt Bodies at Mach Number 3.12," NACA TN 4099, October 1957

(h) Jack, J. R.; Wisniewski, R. J.; and Diaconis, N. S., "Effects of Extreme Surface Cooling on Boundary Layer Transition," NACA TN 4094, October 1957

(i) May, A., and Williams, T. J., "Free-Flight Ranges at the Naval Ordnance Laboratory," NavOrd Report 4063, July 1955

(j) Witt, Jr., W. R., "Free Flight Boundary Layer Transition Studies," Proceedings from the Midwestern Conference on Fluid and Solid Mechanics held at Purdue University, September 1955

(k) Murphy, C. H., "Data Reduction for the Free Flight Spark Ranges," BRL Report 900, February 1954

(l) Eber, G. R., "Recent Investigation of Temperature Recovery and Heat Transmission on Cones and Cylinders in Axial Flow in the NOL Aeroballistics Wind Tunnel," Journal of the Aeronautical Sciences, Vol. 19, No. 1, p. 1, 1952

(m) des Clers, B., and Sternberg, J., "On Boundary-Layer Temperature Recovery Factors," Journal of the Aeronautical Sciences, Vol. 19, No. 9, p. 645, 1952

(n) Stine, H. A., and Scherrer, R., "Experimental Investigation of the Turbulent Boundary Layer Temperature Recovery Factor on Bodies of Revolution at Mach Numbers from 2.0 to 3.8," NACA TN No. 2664, 1952

(o) Staff of the Computing Section, Center of Analysis (under direction of Zdenek Kopal), "Tables of Supersonic Flow Around Yawing Cones," Technical Report No. 3, M.I.T., 1947

(p) Ames Research Staff, "Equations, Tables, and Charts for Compressible Flow," NACA Report 1135, 1953

(q) Jedlicka, J. R.; Wilkins, M. E.; and Seiff, A., "Experimental Determination of Boundary Layer Transition on a Body of Revolution at M = 3.5," NACA TN 3342, October 1954

(r) Braslow, A. L.; Knox, E. C.; and Horton, E. A., "Effect of Distributed Three-Dimensional Roughness and Surface Cooling on Boundary-Layer Transition and Lateral Spread of Turbulence at Supersonic Speeds," NACA TN D-53, October 1959

(s) Smith, A. M. O., and Clutter, D. W., "The Smallest Height of Roughness Capable of Affecting Boundary-Layer Transition," Journal of the Aeronautical Sciences, Vol. 26, No. 4, p. 229, April 1959

(t) Van Driest, E. R., "The Problem of Aerodynamic Heating," Institute of the Aeronautical Sciences, Preprint No. 645, 1956

(u) Van Driest, E. R., "Investigation of Laminar Boundary Layer in Compressible Fluids Using the Crocco Method," NACA TN 2597, 1952

APPENDIX A

Calculation of Surface Temperature Increase Due to Aerodynamic Heating

1. The temperature increase of the cone surface was calculated as follows:

a. The cone was divided into sections as shown in Figure A-1. The temperature and physical properties of the cone were considered constant within each section.

b. At t = 0, the temperature of the cone was assumed to be constant.

c. The aerodynamic heating is estimated by: $q_w = h\,(Tr - Iw)$. The heat transfer coefficient h is obtained from the local skin-friction coefficient through a modified Reynolds-analogy form and the Stanton number defined by $C_H = \dfrac{h}{\rho_e\, U_e\, C_p}$.

d. At time t + Δt, the temperature of each section was determined by the temperature of the adjoining sections at time t, the heat entering the section through its lateral surfaces due to aerodynamic heating, and the heat capacity of the section.

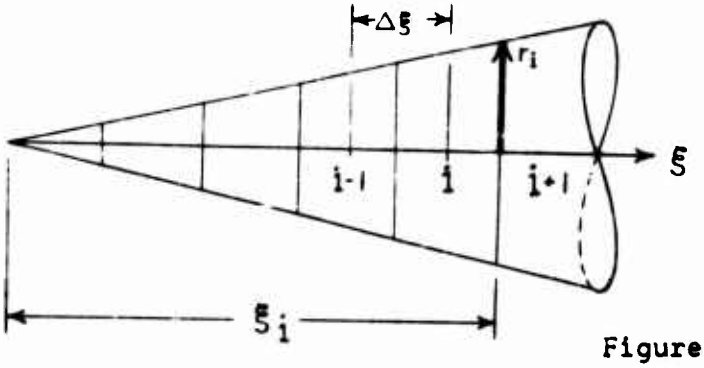

Figure A-1

The heat input to the i^{th} section due to aerodynamic heating is:

$$q_{CV} = \rho_e U_e C_{P_e} A_S C_H (T_r - T_W) \qquad \text{(A-1)}$$

where: A_s = surface area of the i^{th} section.

The heat transferred into the i^{th} section by conduction is:

$$q_{CD} = -k_m A_m \frac{\Delta T}{\Delta \xi} \tag{A-2}$$

where: A_m = cross-sectional area of front or back of i^{th} section

ΔT = temperature difference between center of i^{th} section and center of $i \pm 1^{th}$ section

$\Delta \xi$ = distance between center of sections

The net heat change for the i^{th} section can be expressed as:

$$q_N = \rho_m V_m C_{P_m} \frac{\Delta T}{\Delta t} \tag{A-3}$$

where: V_m = volume of i^{th} section

ΔT = temperature change of i^{th} section during time Δt.

The net heat change for the i^{th} section can also be expressed as:

$$q_{N_i} = q_{CV_i} + q_{CD_i} - q_{CD_{i-1}} \tag{A-4}$$

Referring to equations (A-1), (A-2), and (A-3), equation (A-4) can be written as:

$$\rho_m V_m C_{P_m} \frac{\Delta T}{\Delta t} = \left[\rho_e U_e C_{P_e} A_S C_H (T_r - T_W)\right]_i + \left[k_m A_m \frac{\Delta T}{\Delta \xi}\right]_i - \left[k_m A_m \frac{\Delta T}{\Delta \xi}\right]_{i-1}$$

Solving the above for ΔT gives:

$$\Delta T = \frac{\rho_e C_{P_e} A_{S_i}}{\rho_m C_{P_m} V_{m_i}} U_e C_H (T_r - T_{W_i}) + \frac{k_m}{\rho_m C_{P_m}} \left[\frac{A_{m_i}}{V_{m_i} \Delta \xi}(T_{W_{i-1}} - T_{W_i}) - \frac{A_{m_{i-1}}}{V_{m_i} \Delta \xi}(T_{W_i} - T_{W_{i-1}})\right] \tag{A-5}$$

Equation (A-5) will give the temperature rise for the i^{th} section during a time interval Δt.

2. The following procedure can be used to calculate the temperature distribution along the cone as a function of time. Consider that initially (t = o) the body is at a uniform temperature. For the first increment of time, equation (A-5) reduces to:

$$\Delta T_1 = \frac{\rho_e C_{p_e} A_{s_1}}{\rho_m C_{p_m} V_{m_1}} U_e C_H (T_r - T_W) \Delta t \qquad \text{(A-6)}$$

Since C_H, A_{s_i}, and V_{m_i} are functions of ξ, equation (A-6) will give the temperature distribution along the body at time $t + \Delta t_1$ from the equation:

$$T_{\Delta T_1} = T_{W_{t=0}} + \Delta T_1 \qquad \text{(A-7)}$$

For all time after $t = \Delta t_1$, the temperature rise of each section is given by equation (A-5).

3. The shadowgraph pictures of the cone in flight were observed to determine where laminar and where turbulent values of C_H should be used.

4. The turbulent C_{H_t} was calculated from the local turbulent skin friction coefficient C_{f_t} by means of the Reynolds analogy form:

$$C_{H_t} = \frac{C_{f_t}}{\mathcal{A}\, 2} \qquad \text{(A-8a)}$$

$\mathcal{A}$ was assumed to be 0.825. C_{f_t} was obtained by an iteration process from the following equation (reference (t)):

$$\frac{0.242}{C_{f_t}^{1/2}\left(\frac{\gamma-1}{2}M_e^2\right)^{1/2}}\left(\sin^{-1}\alpha + \sin^{-1}\beta\right) = 0.41 + \log_{10}\left(R_{e_e} C_{f_t}\right) - \omega \log_{10}\left(\frac{T_W}{T_e}\right) \qquad \text{(A-9a)}$$

Where:

$$\alpha = \frac{2A^2 - B}{(B^2 + 4A^2)^{1/2}} \qquad \beta = \frac{B}{(B^2 + 4A^2)^{1/2}}$$

$$A^2 = \frac{\frac{\gamma - 1}{2} M_e^2}{T_w/T_e} \qquad B = \frac{1 + \frac{\gamma - 1}{2} M_e^2}{T_w/T_e} - 1$$

$$\omega = \frac{\log_{10}\left[\left(\frac{T_w + 198.6}{T_e + 198.6}\right)\left(\frac{T_e}{T_w}\right)^{3/2}\right]}{\log_{10}(T_e/T_w)}$$

Although equation (A-9a) applies to a flat plate, the heat transfer coefficient will equal the heat transfer coefficient on a cone at the same local Mach number and same ratio of wall to local free stream temperature if the Reynolds number is divided by two (reference (t)).

5. The laminar C_{H_1} was calculated from the local laminar skin friction coefficient C_{f_1} by means of the Reynolds analogy form:

$$C_{H_1} = \frac{C_{f_1}}{\mathcal{A}\, 2} \qquad \text{(A-8b)}$$

$\mathcal{A}$ was assumed to be 0.925. C_{f_1} was obtained from Figure 4 of reference (u). Since reference (u) applies to a flat plate, the Reynolds number must be divided by three (reference (t)) to make the results applicable to a cone.

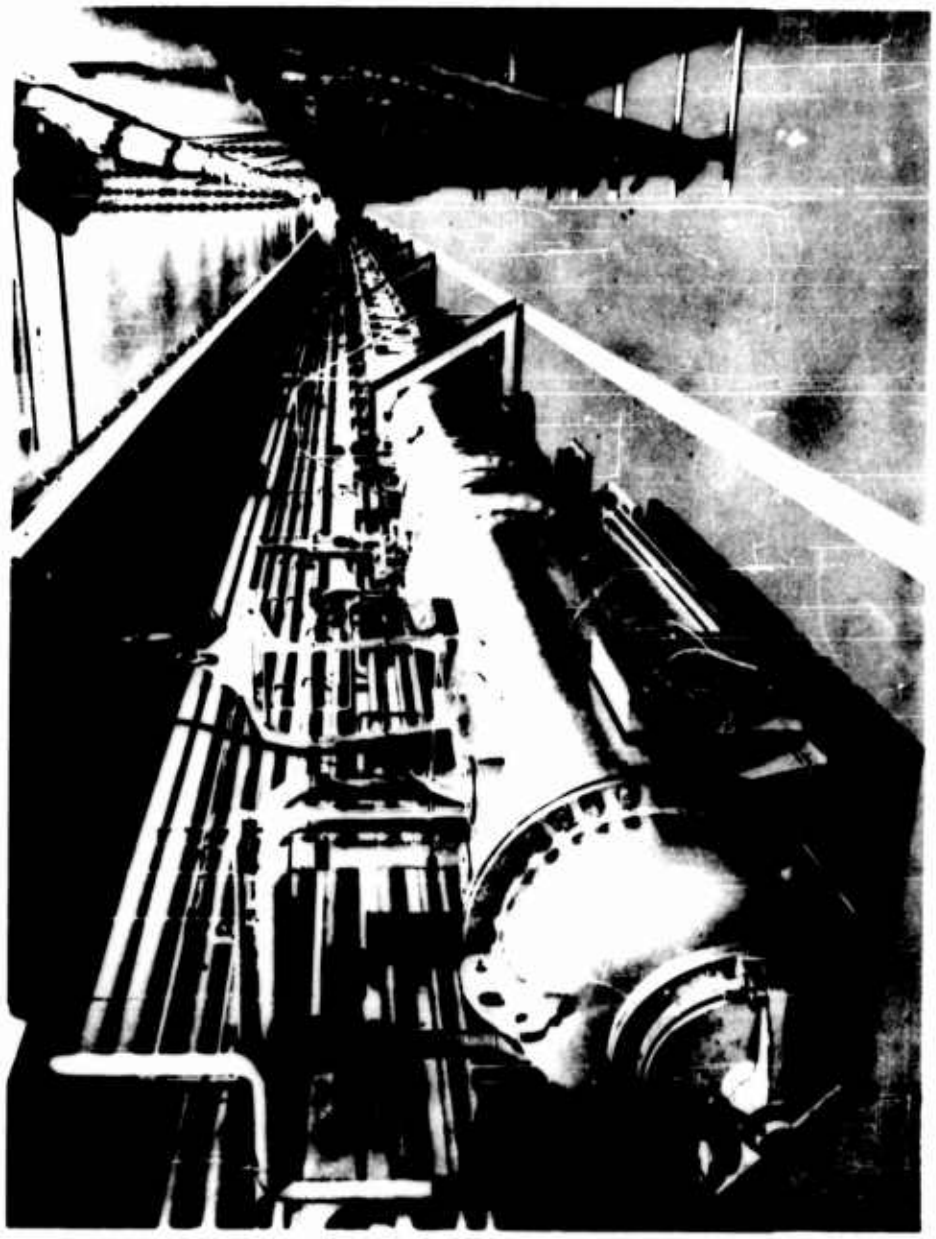

FIG. 1 NOL PRESSURIZED BALLISTICS RANGE

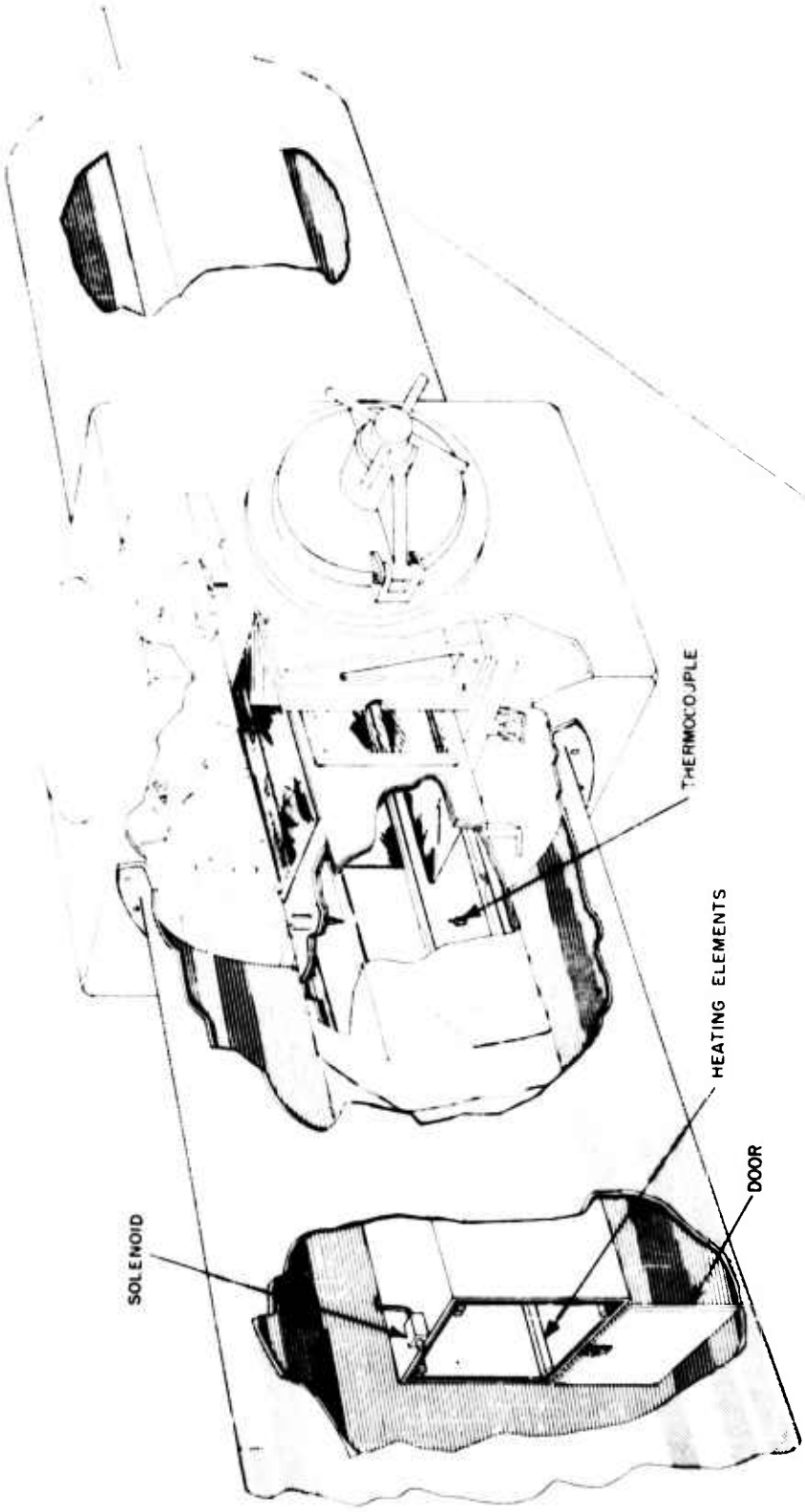

FIG. 2 SKETCH OF HEATING BOX INSTALLED IN BALLISTICS RANGE

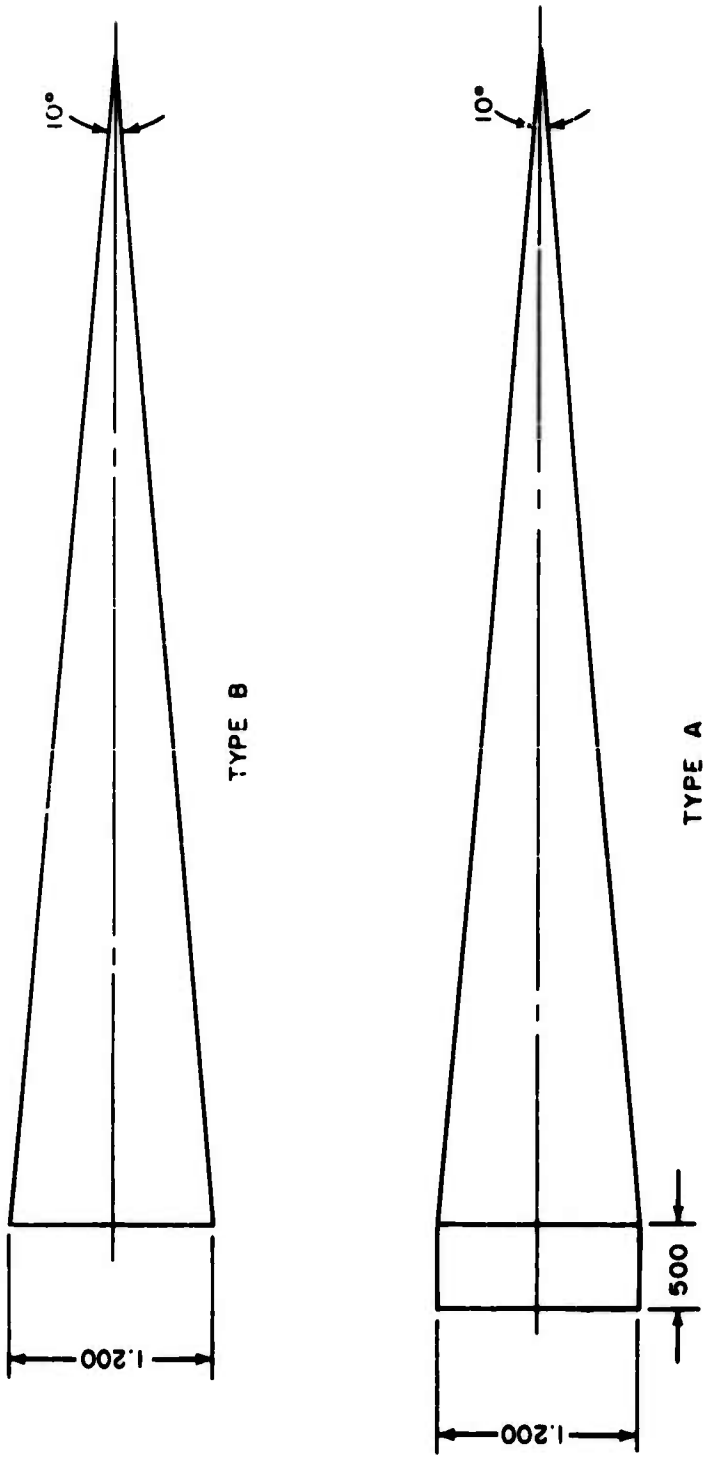

FIG. 3 SKETCH OF MODELS

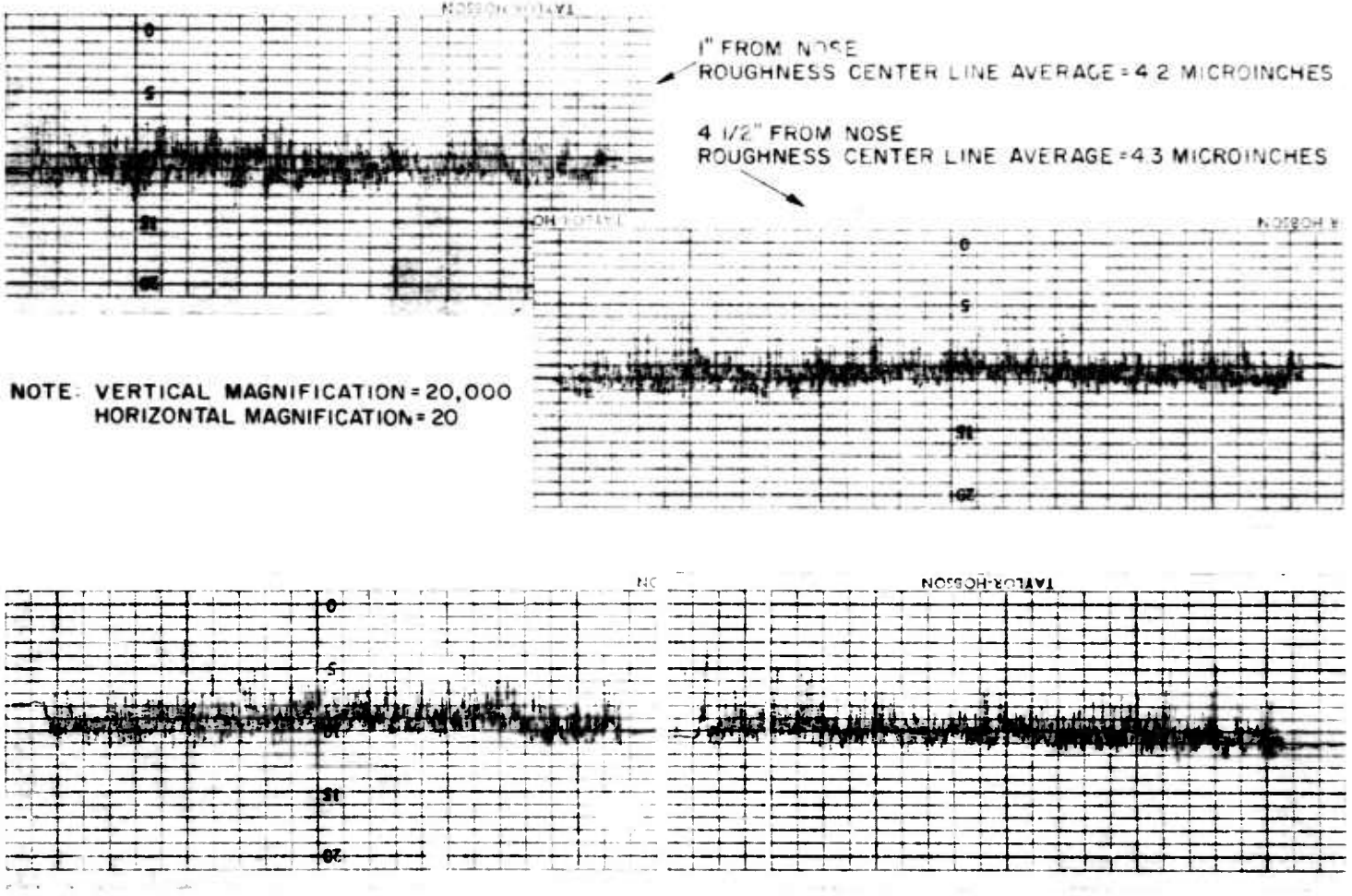

FIG. 4 TYPICAL SURFACE ROUGHNESS MEASUREMENTS

FIG. 5 TRANSITION MODEL NOSE MAGNIFIED 100 TIMES

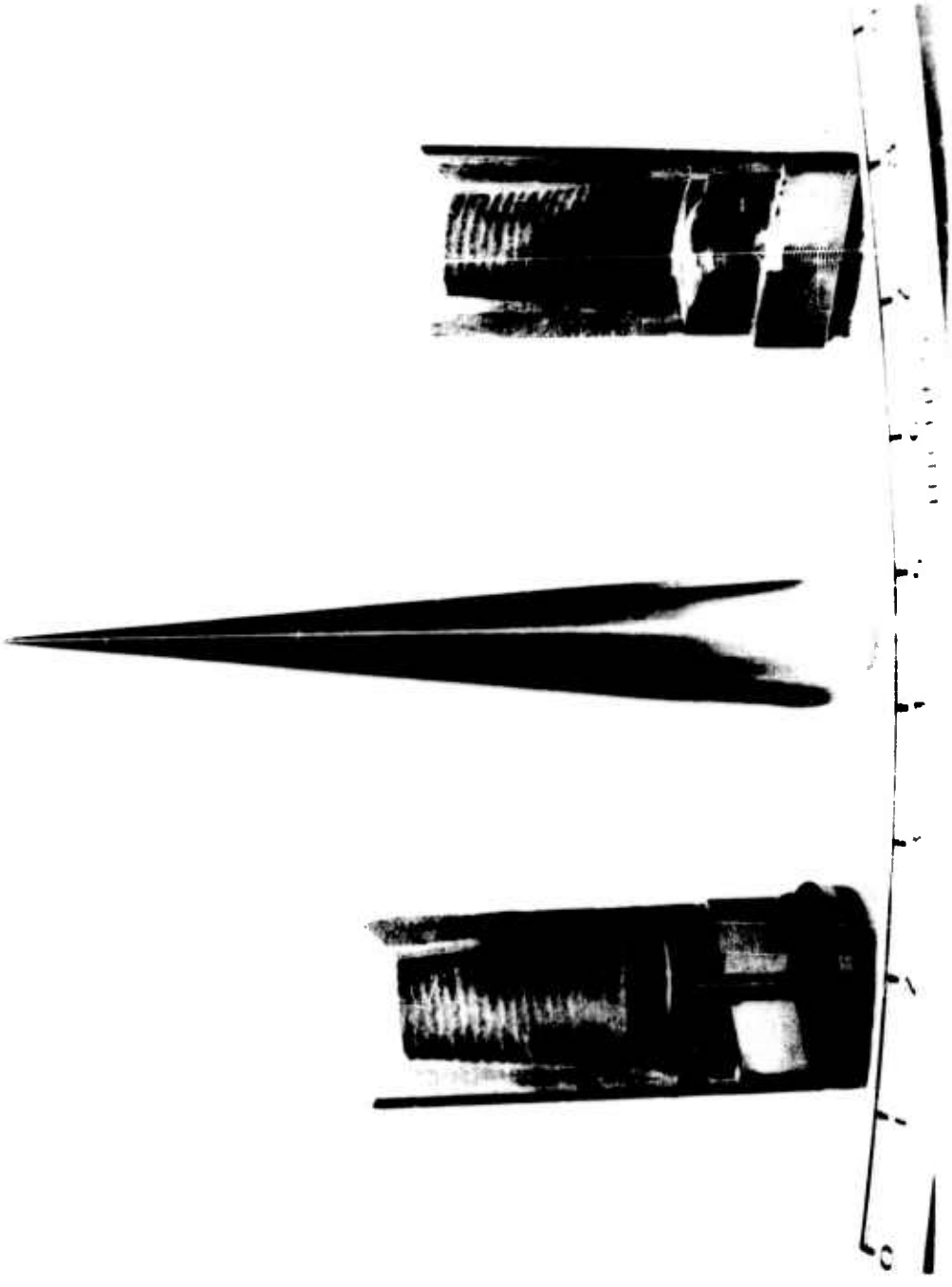

FIG. 6 TYPICAL MODEL AND SABOT

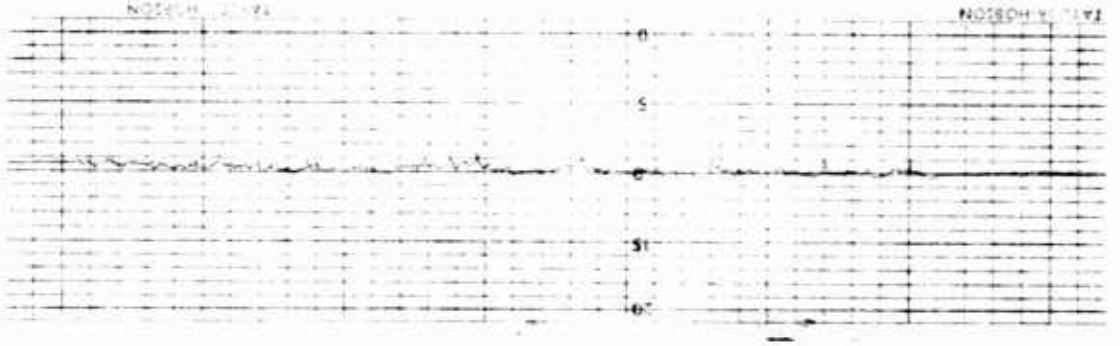

BEFORE ABRASION AND IMPACT TEST

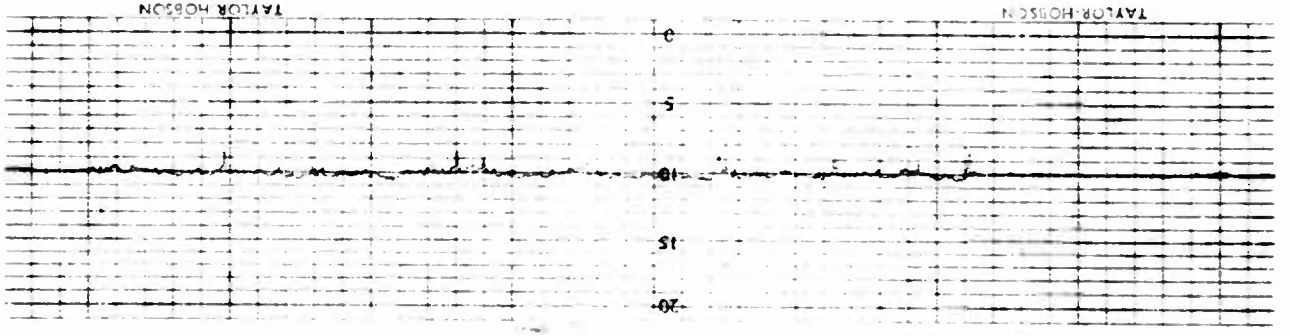

AFTER ABRASION AND IMPACT TEST

NOTE:
VERTICAL MAGNIFICATION 10,000
HORIZONTAL MAGNIFICATION 20

FIG. 7 TALYSURF RECORDS SHOWING THE EFFECT OF SABOT ABRASION AND IMPACT ON A MODEL SURFACE

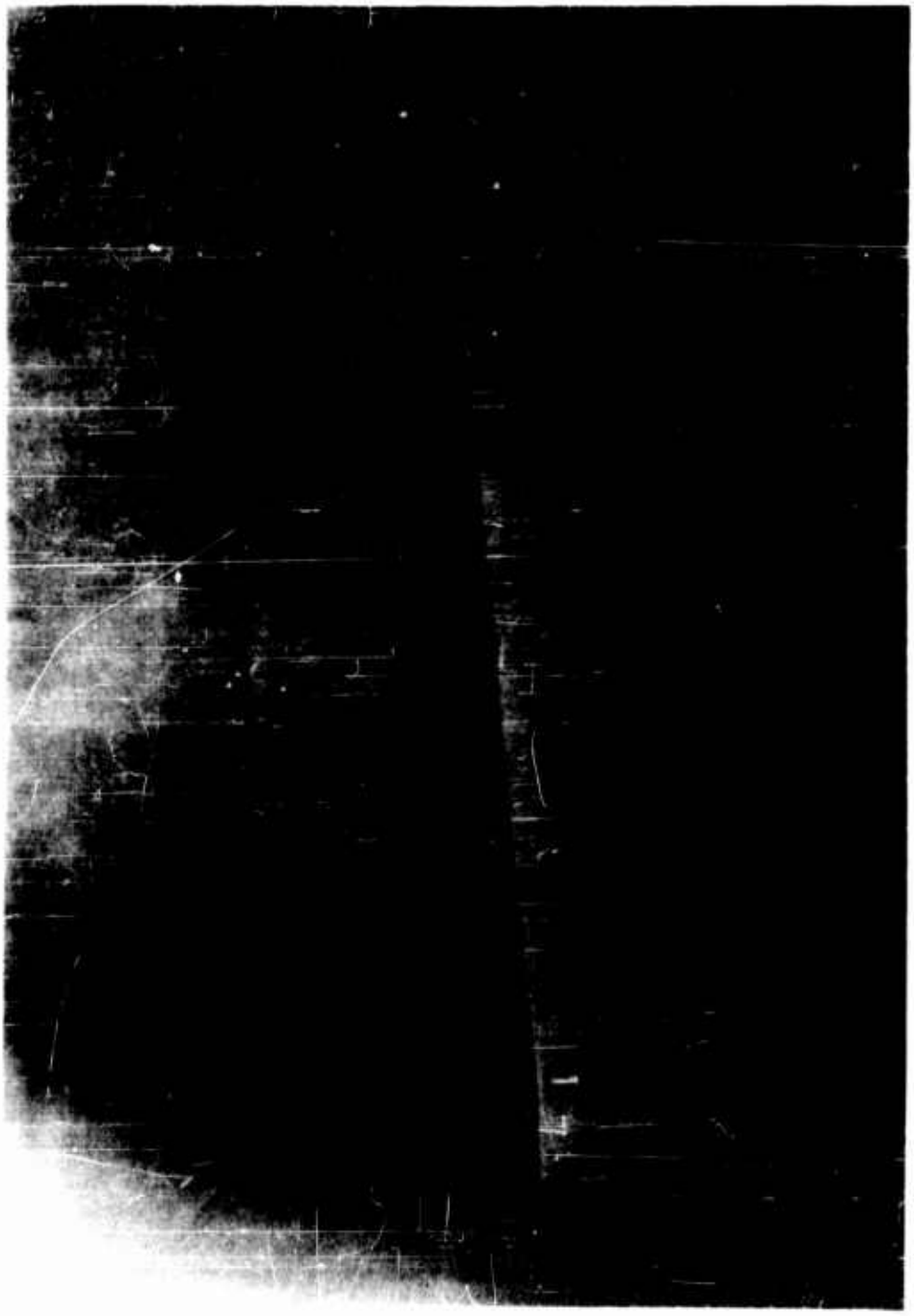

FIG. 8 TYPICAL SPARK SHADOWGRAPH OF TRANSITION MODEL

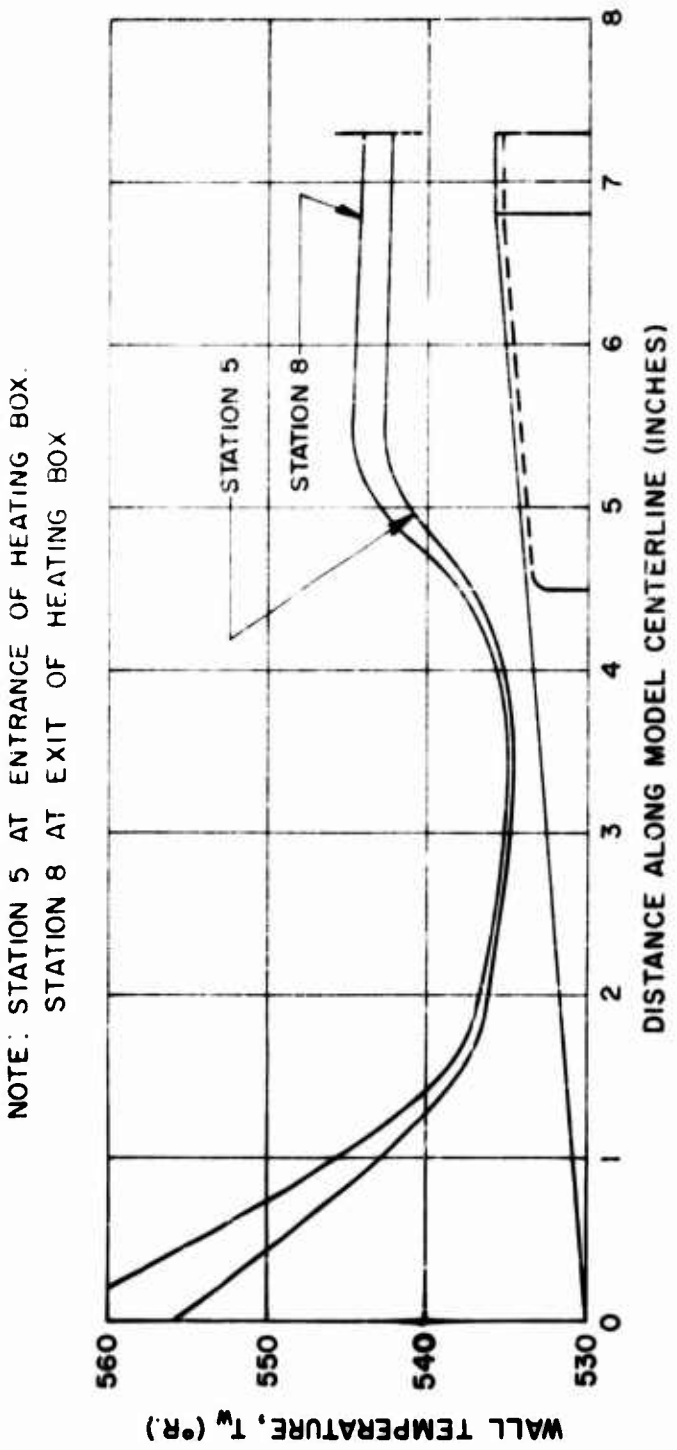

FIG. 9 TYPICAL WALL TEMPERATURE DISTRIBUTIONS ALONG THE LENGTH OF A MODEL.

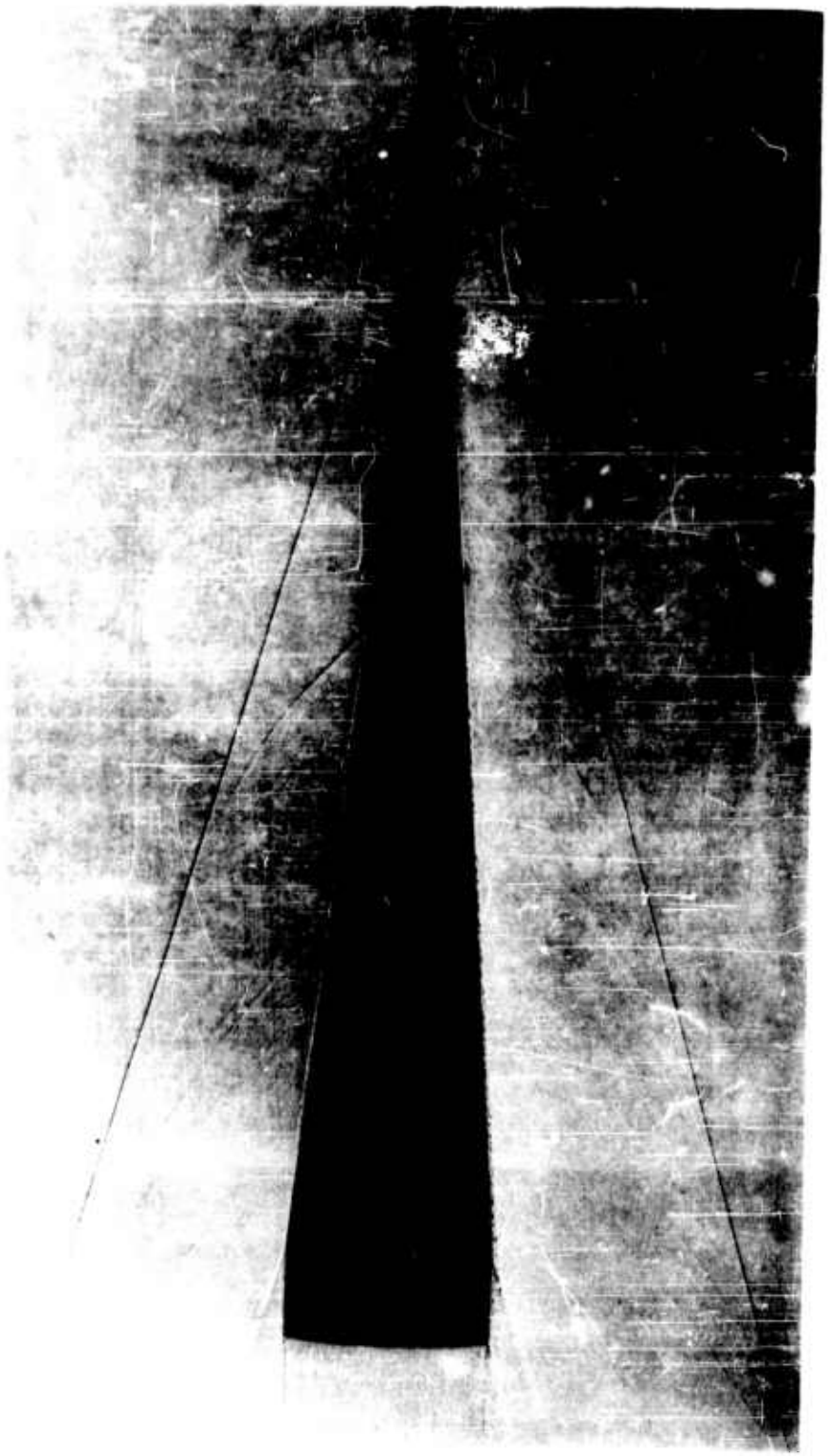

FIG. 10 TURBULENT BURST ON TRANSITION MODEL (ζ_w = 1°)

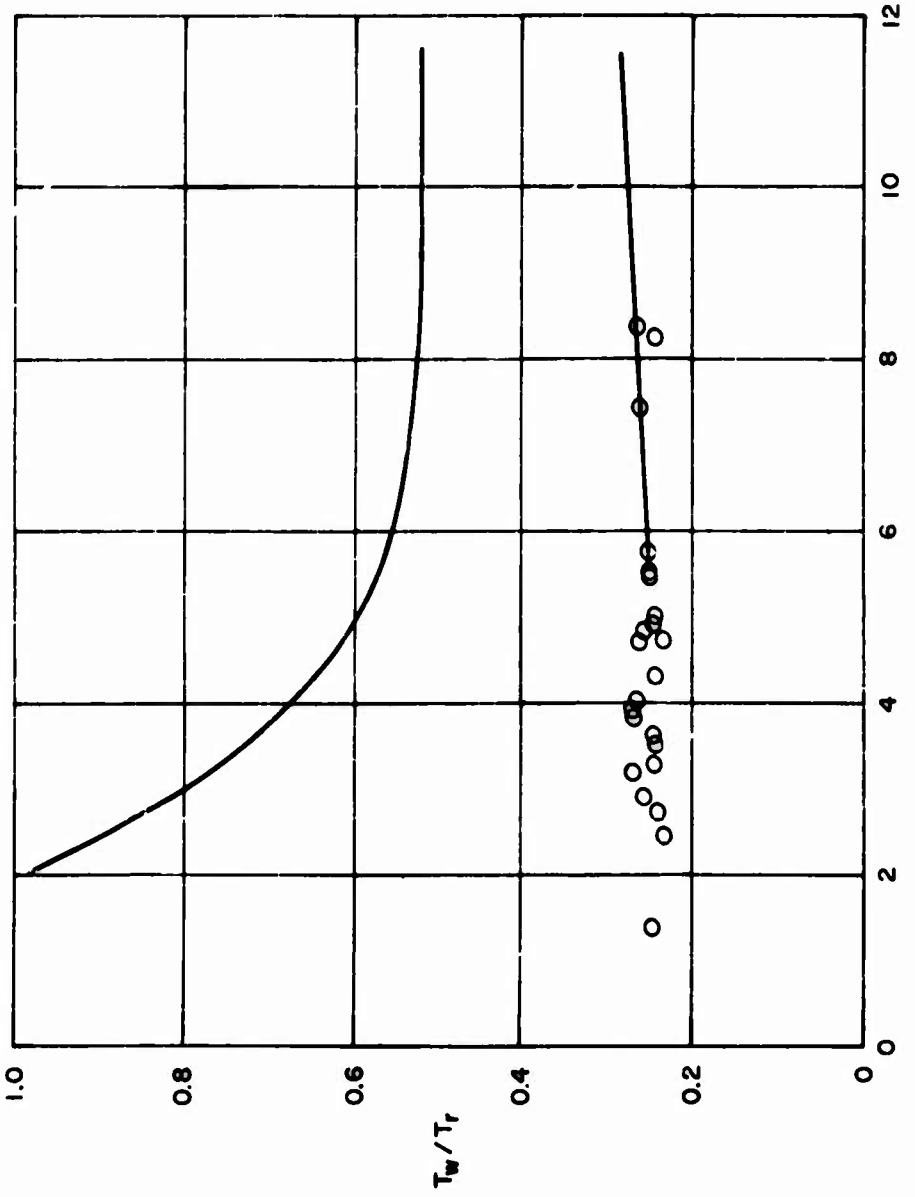

FIG. 11 VARIATION OF LOCAL TRANSITION REYNOLDS NUMBER WITH TEMPERATURE RATIO.

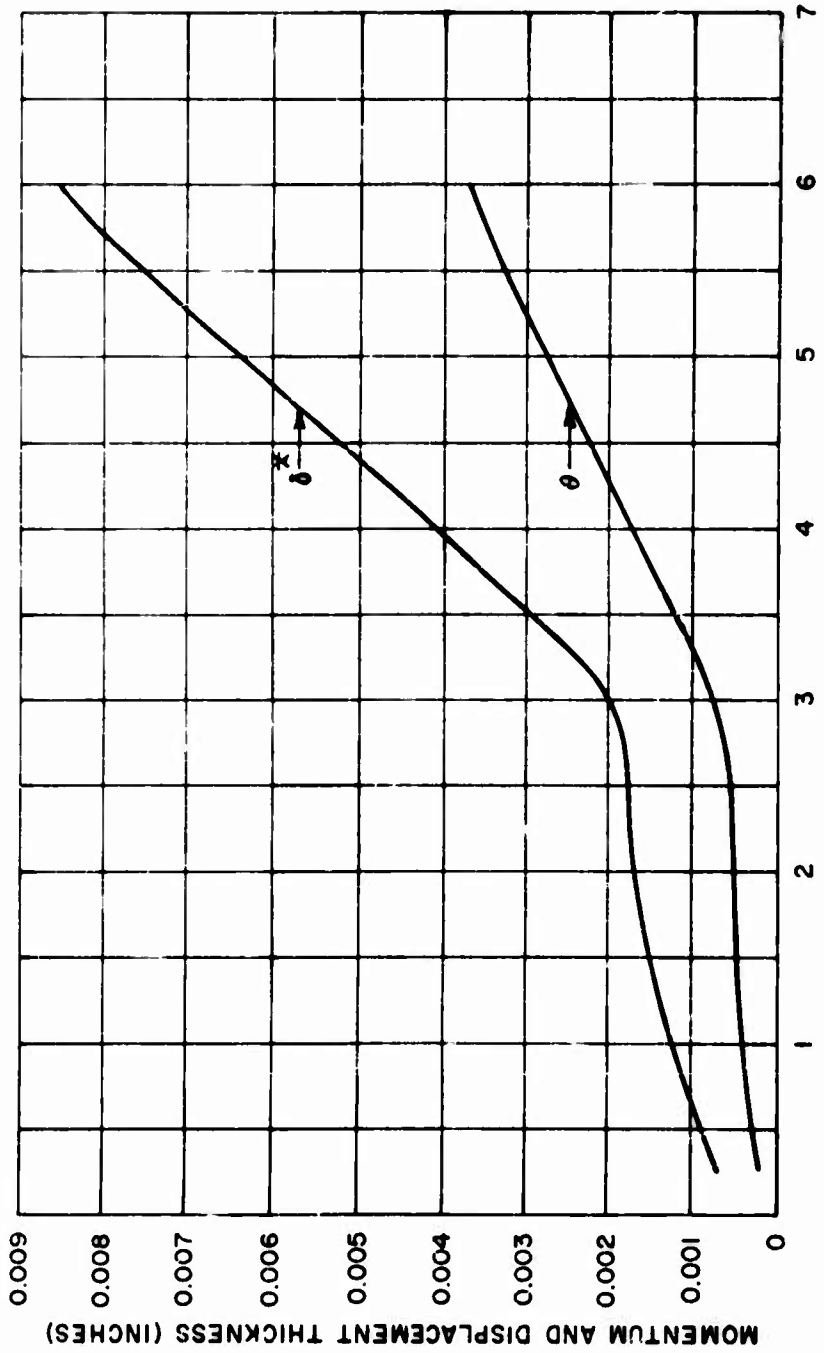

FIG. 12 BOUNDARY LAYER MOMENTUM THICKNESS AND DISPLACEMENT THICKNESS ALONG THE LENGTH OF A MODEL.

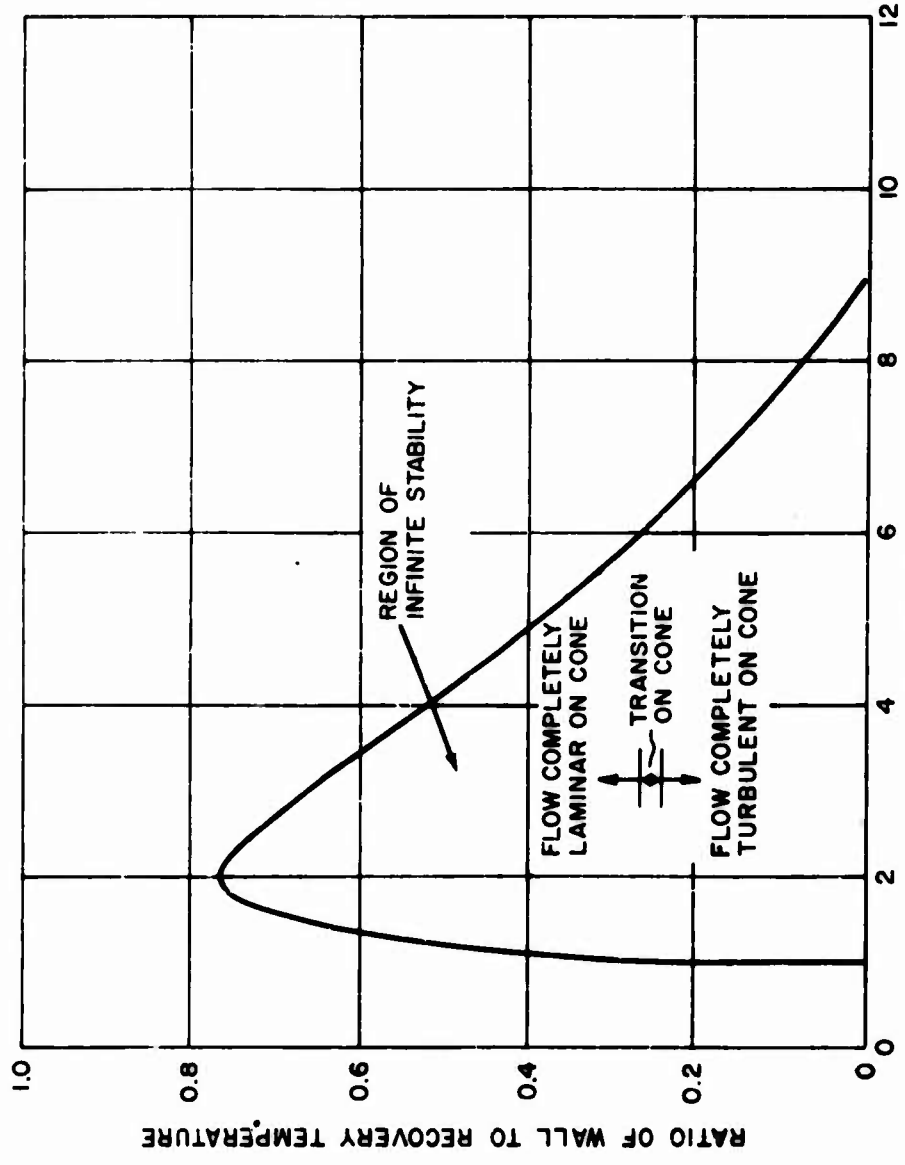

FIG. 13 COOLING REQUIRED FOR COMPLETE STABILIZATION OF THE LAMINAR BOUNDARY LAYER ON A FLAT PLATE.

SHOT NO.	STATION NO.	V FT/SEC.	M	T_{c_R}	P LB/IN.^{2}	T_w/T_r	X_{tr} TOP-FT.	X_{tr} BOTTOM-FT.	FREE-STREAM $Re_{tr} \times 10^{-6}$ TOP	FREE-STREAM $Re_{tr} \times 10^{-6}$ BOTTOM	LOCAL $Re_{tr} \times 10^{-6}$ TOP	LOCAL $Re_{tr} \times 10^{-6}$ BOTTOM	S_v DEG.	S_h DEG.
4046	8	4576	3.24	821	14.49	.234	.428	.179	4.24	2.32	4.72	2.43	-1.83	-1.72
4046	8•	4576	3.24	821	14.49	.234	.238	.131	3.08	1.70	3.43	1.79	-1.83	-1.72
4047	8	4356	3.26	736	11.98	.259	.352	.235	4.32	2.88	4.85	2.98	-3.72	-.80
4047	8•	4356	3.26	736	11.98	.259	----	.159	----	1.95	----	1.95	-3.72	-.80
4048	6	4424	3.21	783	12.14	.248	.456	.456	5.18	5.18	5.76	5.76	.04	-.46
4048	7	4421	3.25	765	12.14	.250	.427	.434	5.04	5.12	5.44	5.49	-.23	.29
4048	7•	4421	3.25	765	12.14	.250	.396	.177	4.70	2.09	5.07	2.24	-.23	.29
4050	6	4293	3.26	714	11.69	.268	all laminar	cannot read	>7.12	----	>8.60	----	-1.8	.23
4050	7	4290	3.25	718	11.69	.268	all laminar		>7.02	>7.02	>8.40	>8.34	-.19	-.41
4050	8	4288	3.26	712	11.69	.269	.174	.280	2.17	3.25	3.14	3.59	1.09	.83
4050	8•	4288	3.26	712	11.69	.269	.118	.146	1.47	1.82	2.13	2.19	1.09	.83
4051	8	4418	3.17	801	13.37	.247	.236	.100	2.84	1.20	3.31	1.38	-.63	.40
4056	6	4443	3.18	806	14.54	.244	.551	>.574	7.17	>7.47	8.25	>8.54	-.18	.80
4056	6•	4443	3.18	806	14.54	.244	----	.294	----	3.83	----	4.38	-.18	.80
4056	7	4440	3.16	815	14.54	.243	.334	.327	4.26	4.17	4.98	4.93	.36	3.44
4056	7•	4440	3.16	815	14.54	.243	.167	----	2.13	----	2.49	----	.36	3.44
4057	5	4266	3.08	784	14.67	.261	all laminar		>8.05	>8.05	>8.12	>8.14	.14	3.04
4057	8	4239	3.09	774	14.67	.264	.303	.289	4.07	3.88	4.04	3.84	-.15	1.78
4057	8•	4239	3.09	774	14.67	.264	.269	.252	3.61	3.38	3.59	3.35	-.15	1.78
4058	6	4266	3.16	758	14.64	.262	.487	.476	6.83	6.68	8.37	7.43	-3.28	-2.98
4058	7	4263	3.14	767	14.64	.261	.435	.302	5.97	4.15	7.43	4.71	-3.17	-1.74
4058	7•	4263	3.14	767	14.64	.261	.302	.147	4.15	2.02	5.15	2.29	-3.17	-1.74
4059	8	4438	3.16	811	14.52	.245	.251	.279	3.22	3.58	3.61	4.31	2.39	-.34
4060	7	4368	2.95	897	15.20	.241	.272	.212	3.02	2.35	3.52	2.73	-.23	-1.43
4060	7•	4368	2.95	897	15.20	.241	.177	.173	1.97	1.92	2.29	2.22	-.23	-1.43

• Transition considered to occur at beginning of the first burst.

TABLE I

DATA OBTAINED FROM TRANSITION MODELS DURING THEIR FLIGHT THROUGH THE HEATING BOX

External Distribution List

	No. of Copies
Chief, Bureau of Naval Weapons Department of the Navy Washington 25, D. C.	
Attn: RMMC	1
Attn: RMGA	1
Attn: RAAA	1
Attn: RRRE	3
Director, Special Projects Department of the Navy Washington 25, D. C.	
Attn: SP-20	4
Attn: SP-27	2
Attn: SP-272	1
Office of Naval Research Room 2709-T-3 Washington 25, D. C.	
Attn: Head, Mechanics Branch	1
Commanding Officer Office of Naval Research Branch Office, Box 39, Navy 100 Fleet Post Office, New York, N.Y.	5
Director, DTMB Aerodynamics Laboratory Washington 7, D. C.	
Attn: Library	1
Commander U. S. Naval Ordnance Test Station China Lake, California	
Attn: Technical Library	1
Director Naval Research Laboratory Washington 25, D. C.	
Attn: Code 2027	1
Attn: Mr. Edward Chapin, Code 6310	1
Naval Weapons Laboratory Dahlgren, Virginia	
Attn: Library	1
NASA Ames Research Center Moffett Field, California	
Attn: Librarian	1

External Distribution List

	No. of Copies
NASA Langley Research Center Langley Field, Virginia	
Attn: Librarian	1
Attn: C. H. McLellan	1
Attn: J. J. Stack	1
Attn: Adolf Busemann	1
Attn: Rodger W. Peters (Structures Res. Div.)	1
Attn: Russell Hopko, PARD	1
NASA Lewis Research Center 21000 Brookpart Road Cleveland, Ohio	
Attn: Chief, Propulsion Aerodynamics Div.	1
Attn: Mr. George Mandel, Chief, Library	2
Office of the Assistant Secretary of Defense (R&D) Room 3E1041, The Pentagon Washington 25, D. C.	
Attn: Library (Technical)	1
Research and Development Board Room 3D1041, The Pentagon Washington 25, D. C.	
Attn: Library	2
ASTIA Arlington Hall Station Arlington 12, Virginia	
Attn: TIPDR	10
Commander, NMC Point Mugu, California	
Attn: Technical Library	1
Commanding General Aberdeen Proving Ground, Md.	
Attn: Technical Information Branch	1
Attn: Ballistics Research Laboratories	1
Director of Intelligence Headquarters, USAF Washington 25, D. C.	
Attn: AFOIN-3B	1

External Distribution List

	No. of Copies
Commander Wright Air Development Division Wright-Patterson Air Force Base, Ohio	
Attn: WCOSI-3	2
Attn: WCLSW-5	1
Attn: WCRRD	3
Commander, AFBMD Air Research & Development Command P. O. Box 262 Inglewood, California	
Attn: WDTLAR	1
Attn: WDTVR	2
Chief, DASA The Pentagon Washington, D. C.	
Attn: Document Library	1
Commanding General Arnold Engineering Development Center Tullahoma, Tennessee	
Attn: Technical Library	1
Attn: AEKS	5
Commanding Officer, DOFL Washington 25, D. C.	
Attn: Library Rm. 211, Bldg. 92	1
NASA George C. Marshall Space Flight Center Huntsville, Alabama	
Attn: M-S&M-PT (Mr. H. A. Connell)	5
Attn: Dr. W. R. Lucas (M-SFM-M)	1
Attn: Dr. Ernst Geissler	1
Office, Chief of Ordnance Department of the Army Washington 25, D. C.	
Attn: ORDTU	1
Aerospace Corporation El Segundo, California	
Attn: Dr. Bitondo	1

External Distribution List

	No. of Copies
APL/JHU 8621 Georgia Avenue Silver Spring, Maryland	
Attn: Tech. Reports Group	2
Attn: Dr. D. Fox	1
Attn: Dr. Freeman Hill	1
Attn: Dr. L. L. Cronvich	1
Attn: Librarian (Via: BUWEPSREP)	1
AVCO Manufacturing Corporation Research & Advanced Development Division 201 Lowell Street Wilmington, Massachusetts	
Attn: Mr. J. P. Wamser	1
AVCO Manufacturing Corporation Everett, Massachusetts	
Attn: Dr. Kantrowitz	1
General Electric Company Space Vehicle & Missiles Department 21 South 12th Street Philadelphia, Pennsylvania	
Attn: Dr. J. Stewart	1
Attn: Dr. Otto Klima	1
Attn: Mr. E. J. Nolan	1
Attn: Mr. L. McCreight	1
General Electric, Research Laboratory 3198 Chestnut Street Philadelphia, Pennsylvania	
Attn: Dr. Leo Steg	1
National Aeronautics and Space Administration 1520 H Street, N.W. Washington, D. C.	5
NASA High Speed Flight Station Edwards Field, California	
Attn: W. C. Williams	1
Oak Ridge National Laboratory P. O. Box E Oak Ridge, Tennessee	
Attn: Mr. W. D. Manly	1

External Distribution List

	No. of Copies
Lockheed Aircraft Corporation Missiles and Space Division P. O. Box 504 Sunnyvale, California Attn: Dr. L. H. Wilson	1
Via: BUWEPSREP P. O. Box 504 Sunnyvale, California	
Lockheed Aircraft Corporation Research Laboratory Palo Alto, California Attn: W. Griffith	1
Via: BUWEPSREP P. O. Box 504 Sunnyvale, California Attn: SpL-314	1
Atomic Energy Commission Engineering Development Branch Division of Reactor Development Headquarters, US AEC Washington 25, D. C.	
Attn: Mr. J. M. Simmons	1
Attn: Mr. M. J. Whitman	1
Attn: Mr. J. Conners	1
University of California Lawrence Radiation Laboratory P. O. Box 808 Livermore, California	
Attn: Mr. W. M. Wells, Propulsion Division	1
Attn: Mr. Carl Kline	1
Polytechnic Institute of Brooklyn 527 Atlantic Avenue Freeport, New York	
Attn: Dr. Paul A. Libby	1
Via: Commanding Officer Office of Naval Research Branch Office 346 Boradway New York 13, New York	
General Applied Sciences Laboratories, Inc. Merrick and Stewart Avenues East Meadow, New York	
Attn: Mr. Robert Byrne	1

NOLTR 61-83

External Distribution List

	No. of Copies
Jet Propulsion Laboratory 4800 Oak Grove Drive Pasadena 3, California	
Attn: I. R. Kowlan, Chief, Reports Group	1
Attn: Dr. L. Jaffee	2
Los Alamos Scientific Laboratory P. O. Box 1663 Los Alamos, New Mexico	
Attn: Dr. Donald F. MacMillan N-1 Group Leader	1
Institute for Defense Analyses Advanced Research Projects Agency Washington 25, D. C.	
Attn: Mr. W. G. May General Sciences Branch	1
Kaman Aircraft Corporation Nuclear Division Colorado Springs, Colorado	
Attn: Dr. A. P. Bridges	1
U. S. Atomic Energy Commission P. O. Box 62 Oak Ridge, Tennessee	
Attn: TNI:NLP:ATD:10-7	1
Sandia Corporation Livermore Laboratory P. O. Box 969 Livermore, California	1
United Aircraft Corporation Research Laboratories East Hartford 8, Connecticut	
Attn: Mr. H. J. Charette	1
Attn: Mr. H. Taylor	1
Sandia Corporation Sandia Base Albuquerque, New Mexico	
Attn: Mr. Alan Pope	1
Defense Metals Information Center Battelle Memorial Institute 505 King Avenue Columbus 1, Ohio	1

NOLTR 61-83

External Distribution List

	No. of Copies
Commanding General Army Rocket and Guided Missile Agency Redstone Arsenal, Alabama Attn: John Morrow	1
National Bureau of Standards Washington 25, D. C. Attn: Dr. Galen B. Schubauer	1
Cornell Aeronautical Laboratory 4455 Genesee Street Buffalo, New York Attn: Dr. Gordon Hall	1
Department of Mechanical Engineering University of Delaware Newark, Delaware Attn: Dr. James P. Hartnett	1
National Aeronautics and Space Administration 1520 H Street, N.W. Washington, D. C. Attn: Dr. H. H. Kurzweg	1
Department of Aeronautical Engineering Cornell University Ithaca, New York Attn: Dr. S. F. Shen	1
Department of Aeronautical Engineering University of Maryland College Park, Maryland Attn: A. W. Sherwood	1
NASA Goddard Space Flight Center Greenbelt, Maryland Attn: W. R. Witt, Jr.	1

Naval Ordnance Laboratory, White Oak, Md. (NOL technical report 61-83)
FREE FLIGHT EXPERIMENTAL INVESTIGATIONS OF THE EFFECT OF BOUNDARY LAYER COOLING ON TRANSITION (U), by W.C. Lyons, jr. and N.W. Sheetz, jr. 29 Sept. 1961. 21p. illus., charts, tables, diagrs. (Ballistic research report 46). Task 803-767/73001/03-073.
UNCLASSIFIED

Free flight tests have been conducted in the NOL pressurized ballistics range no. 3 for the purpose of investigating boundary layer transition under the conditions of extreme boundary layer cooling. The tests were conducted on smooth, sharp-nosed, slender cones. The tests were conducted at a nominal Mach number of 3 and a free stream unit Reynolds number per foot of 11.8 x 10^6. The ratio of wall to adiabatic recovery temperature varied between 0.22 and 0.27.
Abstract card is unclassified

1. Bodies - Boundary layer
2. Bodies - Flight tests
3. Boundary layer - Transition
4. Boundary layer - Cooling
I. Title
II. Lyons, W. Carson, jr.
III. Sheetz, Norman W., jr. jt. author
IV. Series
V. Project

Naval Ordnance Laboratory, White Oak, Md. (NOL technical report 61-83)
FREE FLIGHT EXPERIMENTAL INVESTIGATIONS OF THE EFFECT OF BOUNDARY LAYER COOLING ON TRANSITION (U), by W.C. Lyons, jr. and N.W. Sheetz, jr. 29 Sept. 1961. 21p. illus., charts, tables, diagrs. (Ballistic research report 46). Task 803-767/73001/03-073.
UNCLASSIFIED

Free flight tests have been conducted in the NOL pressurized ballistics range no. 3 for the purpose of investigating boundary layer transition under the conditions of extreme boundary layer cooling. The tests were conducted on smooth, sharp-nosed, slender cones. The tests were conducted at a nominal Mach number of 3 and a free stream unit Reynolds number per foot of 11.8 x 10^6. The ratio of wall to adiabatic recovery temperature varied between 0.22 and 0.27.
Abstract card is unclassified

1. Bodies - Boundary layer
2. Bodies - Flight tests
3. Boundary layer - Transition
4. Boundary layer - Cooling
I. Title
II. Lyons, W. Carson, jr.
III. Sheetz, Norman W., jr. jt. author
IV. Series
V. Project

Naval Ordnance Laboratory, White Oak, Md.
(NOL technical report 61-83)
FREE FLIGHT EXPERIMENTAL INVESTIGATIONS OF THE EFFECT OF BOUNDARY LAYER COOLING ON TRANSITION (U), by W.C. Lyons, jr. and N.W. Sheetz, jr. 29 Sept. 1961. 21p. illus., charts, tables, diagrs. (Ballistic research report 46). Task 803-767/73001/03-073.
UNCLASSIFIED

Free flight tests have been conducted in the NOL pressurized ballistics range no. 3 for the purpose of investigating boundary layer transition under the conditions of extreme boundary layer cooling. The tests were conducted on smooth, sharp-nosed, slender cones. The tests were conducted at a nominal Mach number of 3 and a free stream unit Reynolds number per foot of 11.8 x 10^6. The ratio of wall to adiabatic recovery temperature varied between 0.22 and 0.27. Abstract card is unclassified

1. Bodies - Boundary layer
2. Bodies - Flight tests
3. Boundary layer - Transition
4. Boundary layer - Cooling
I. Title
II. Lyons, W. Carson, jr.
III. Sheetz, Norman W., jr. jt. author
IV. Series
V. Project

Naval Ordnance Laboratory, White Oak, Md.
(NOL technical report 61-83)
FREE FLIGHT EXPERIMENTAL INVESTIGATIONS OF THE EFFECT OF BOUNDARY LAYER COOLING ON TRANSITION (U), by W.C. Lyons, jr. and N.W. Sheetz, jr. 29 Sept. 1961. 21p. illus., charts, tables, diagrs. (Ballistic research report 46). Task 803-767/73001/03-073.
UNCLASSIFIED

Free flight tests have been conducted in the NOL pressurized ballistics range no. 3 for the purpose of investigating boundary layer transition under the conditions of extreme boundary layer cooling. The tests were conducted on smooth, sharp-nosed, slender cones. The tests were conducted at a nominal Mach number of 3 and a free stream unit Reynolds number per foot of 11.8 x 10^6. The ratio of wall to adiabatic recovery temperature varied between 0.22 and 0.27. Abstract card is unclassified

1. Bodies - Boundary layer
2. Bodies - Flight tests
3. Boundary layer - Transition
4. Boundary layer - Cooling
I. Title
II. Lyons, W. Carson, jr.
III. Sheetz, Norman W., jr. jt. author
IV. Series
V. Project